

Exact Discrete-Time Implementation of the Mackey–Glass Delayed Model

Pablo Amil, Cecilia Cabeza, and Arturo C. Marti

Abstract—The celebrated Mackey–Glass (MG) model describes the dynamics of physiological *delayed* systems, in which the actual evolution depends on the values of the variables at some *previous* times. This kind of system is usually expressed by delayed differential equations, which turn out to be infinite dimensional. In this brief, an electronic implementation mimicking the MG model is proposed. New approaches for both the nonlinear function and the delay block are made. Explicit equations for the actual evolution of the implementation are derived. Simulations of the original equation, the circuit equation, and experimental data show great concordance.

Index Terms—Chaos, delayed circuits, Mackey–Glass (MG).

I. INTRODUCTION

IN 1977, a paper entitled *Oscillation and Chaos in Physiological Control Systems* [1] was published. It dealt with physiological processes, mainly respiratory and hematopoietic (i.e., formation of blood cellular components) diseases, in which time delays play a significant role. In effect, in the production of blood cells is a considerable delay between the initiation of cellular production in the bone marrow and the release into the blood. Generally, in these processes, the evolution of the system at a given time depends not only on the state of the system at the current time but also on the state of the system at *previous* times.

In their pioneering paper, the Mackey–Glass (MG) model showed that a variety of physiological systems can be adequately described, in terms of simple nonlinear delay-differential equations (DDEs). The model proposed by MG exhibits a wide range of behaviors, including periodic and chaotic solutions. The importance of the MG model lies in the fact that the onset of some diseases is associated with alterations in the periodicity of certain physiological variables, e.g., irregular breathing patterns or fluctuations in peripheral blood cell counts [2].

The dynamics of processes involving time delays, such as those studied by MG, is far more complex than that of nondelayed, i.e., instantaneous, systems. If the dynamics of a system at time t depends on the state of the system at a previous time $t - \tau$, the information needed to predict the evolution is contained in the entire interval $(t - \tau, t)$. Thus, the evolution of a delayed system depends on *infinite* previous values of the variables. Mathematically, delayed systems are modeled in terms of

DDEs, and one single DDE is equivalent to infinite ordinary differential equations (ODEs). Due to their infinite dimensionality, the accuracy of numerical simulations of DDEs is particularly delicate. In practice, this problem is avoided, considering large transients. However, there persist doubts about the stability and accuracy of the methods used to numerically integrate DDEs.

Due to its richness in behaviors, the MG model has acquired relevance of its own [3]–[5]. One frequent application is to use the MG model as a simple way to generate a high-dimensional chaotic signal (see, for example, [6]), which can be helpful to characterize strange attractors using the Kolmogorov entropy, for instance, and, at the end, as a way to distinguish between deterministic chaos and random noise. Other applications could be the employment of the output of the MG model to check the effectiveness of a control or stabilization scheme [7]. The MG model was also proposed in the context of forecasting chaotic data [8], or nonlinear estimation problems [9].

Another possible application of the MG model is to employ several delayed values of the variable $x(t - \tau_1)$, $x(t - \tau_2)$, $x(t - \tau_3)$, . . . instead of only one [4], [10]. More specifically, Tateno and Uchida [10] investigated the generation of chaos in an MG electronic circuit with two time-delayed feedback loops observing different dynamical behaviors when the two delay times were changed. The ratio of the two time delays was found crucial to enhance or suppress the chaotic dynamics. The synchronization of chaos in unidirectionally coupled MG electronic circuits with two time delays was also investigated [4], confirming that synchronization of chaos can be achieved even in the presence of the two time-delayed feedback loops. High-quality synchronization of chaos can be achieved at the strong coupling strengths and parameter-matching conditions between the two circuits.

At present, the interest in the MG still holds. In the context of respiratory diseases, the relevance of the MG model has been recently remarked [11], [12]. In nonlinear science, the lag synchronization of two uncoupled double MG systems has been recently demonstrated in [13]. The prediction of chaotic MG time series is attempted using fuzzy logic in [14] or applied to machine-learning methods [15].

Several electronic implementations of the MG model were reported [10], [16]–[20]. In [16], an electronic implementation based on an *analog delay line* was proposed to address the problem of controlling high-dimensional chaos in infinite-dimensional systems. The analog delay line can be thought as a chain of masses and springs and, broadly speaking, generates an effective delay for frequencies low enough. The same electronic implementation was considered in [17] and [18], to investigate the generalized synchronization and communication between two analog MG circuits. This approach was extended in the design proposed in [19], to analyze the synchronization of multiple delay feedback systems.

Manuscript received November 26, 2014; revised February 4, 2015; accepted March 13, 2015. Date of publication March 23, 2015; date of current version June 25, 2015. This brief was recommended by Associate Editor T. S. Gotarredona.

The authors are with the Physics Institute, Universidad de la República, Iguá, Montevideo 4225, Uruguay. (e-mail: pamil@fisica.edu.uy; cecilia@fisica.edu.uy; marti@fisica.edu.uy)

Color versions of one or more of the figures in this brief are available online at <http://ieeexplore.ieee.org>.

Digital Object Identifier 10.1109/TCSII.2015.2415651

Digital electronic implementations of other delayed systems have been recently proposed in [20]. In this approach, which uses programmable hardware, it is necessary to convert the signal from the RC circuit to the digital domain, apply the delay, and convert back to the analog domain.

The goal of this brief is to propose a novel electronic implementation of the MG system, in which the delay and the nonlinear function are constructed in such a way that exact equations of the circuit evolution may be written. Section II deals specifically with the design of the circuit, paying special attention to the delay block and the function block. In Section III, we derive the governing equation of the designed circuit and show how this implementation approximates the original equation. Then, in Section IV, we compare results of simulations with the original MG equation and the effective circuit equation with the experimental data, which all show great agreement between each other. Finally, in Section V, we draw our conclusions.

II. MODEL AND ITS ELECTRONIC IMPLEMENTATION

Let us consider the production of white blood cells, or *leukocytes*, whose density is denoted by P . According to [1, (Eq. 4b)],

the evolution of the population is governed by a DDE

$$\frac{dP}{dt} = \frac{\beta_0 \Theta^n P_\tau}{\Theta^n + P_\tau^n} - \gamma P \quad (1)$$

where $P_\tau(t) = P(t - \tau)$. The first term in the right-hand side corresponds to the production of blood cells, where parameters β_0 , Θ , and n are related to the production rate, while in the second term, γ determines the decay rate of the cells. To simplify (1), we reduce it to an equivalent equation with less model parameters. To that end, we will define a new state variable and a new independent variable as $x = P/\Theta$ and $t' = \gamma t$, respectively. We also define new parameters, such that $\Gamma = \gamma\tau$ and $\alpha = \beta_0/\gamma$. Thus, (1) can be now written as

$$\frac{dx}{dt'} = \alpha \frac{x_\Gamma}{1 + x_\Gamma^n} - x \quad (2)$$

being $x_\Gamma(t') = x(t' - \Gamma)$. The electronic implementation will mimic this equation by properly setting α and Γ . The exponent n considered in [1] was $n = 10$; however, similar behaviors can be seen with other values [3].

The time delay τ plays a crucial role in the dynamics of the MG model. For the instantaneous system, i.e., $\tau = 0$, depending on the parameter values, there is only one positive stable fixed point. However, as τ is increased, the initially stable equilibrium point becomes unstable, and periodic solutions appear [7]. If τ is further increased, a sequence of bifurcations gives place to oscillations with higher periods and aperiodic behavior. An exhaustive analysis, showing the occurrence of a sequence of Hopf bifurcations and determining the stability of the bifurcating periodic solutions, is presented in [5]. In [3], the presence of continuous deformations of the waveforms is remarked, which create and destroy peaks, resulting in the appearances or disappearances of branches in the bifurcation diagrams, which are considerably more complex than in non-delayed systems, such as those shown in Section V.

The electronic implementation was divided in two main parts: the delay block, which presents only a time shift between

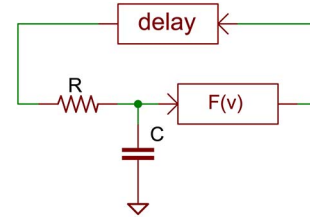


Fig. 1. Block schematic of the complete circuit.

its input and its output; and the function block, which implements the nonlinear term of the equation. The complete circuit looks as in Fig. 1. In this scheme, the function block implements the production term in (1) [or (2)] without delay, i.e.,

$$f(v) = \beta \frac{v}{\theta^n + v^n} \quad (3)$$

and the delay block approximates the transfer function as

$$v_{\text{out}}(t) = v_{\text{in}}(t - \tau). \quad (4)$$

Assuming the ideal behavior of both blocks, the equation for the potential at the capacitor terminals is given by

$$\frac{dv_c(t)}{dt} = \frac{1}{RC} [f(v_c(t - \tau)) - v_c(t)] \quad (5)$$

which can be identified with (2), by setting $t' = t/RC$, $x = v_c/\theta$, $\Gamma = \tau/RC$, and $\alpha = \beta/\theta^n$.

The purpose of the delay block is to copy the input to the output after some time delay. The implementation of this block with analog electronics is possible using a bucket-brigade device (BBD), which is a discrete-time analog device. Internally, it consists of an array of N capacitors, in which the signal is moved along one step at each clock cycle. In our implementation, we used the integrated circuits MN3011 and MN3101 as BBD and clock signal generator, respectively.

The present approach to implement the time delay approximates the desired transfer function given, in this case by (4), by sampling the input signal and outputting their samples N clock periods later. The effective transfer equation read as

$$v_{\text{out}}(t) = g_d v_{\text{in}} \left(T_s \left\lfloor \frac{t}{T_s} - N + 1 \right\rfloor \right) + V_d \quad (6)$$

where T_s , g_d and V_d stand for the sampling period, gain, and offset voltage introduced by the BBD, respectively. In the MN3011, the sampling period can vary between 5 and 50 μs , and N can be selected among the values provided by the manufacturer (i.e., 396, 662, 1194, 1726, 2790, and 3328). An example of its functionality is shown in Fig. 2, where, to fully appreciate the input and output signals, the offset and the gain are null, and a simulated value of N (not provided by the manufacturer) is employed.

In order to avoid the effects of offset and gain, and also to expand the intrinsic dynamic range of the BBD (originally between 0 and 4 V), the delay block includes pre- and postamplification, as well as offset adjustment, as shown in Fig. 3. The delay was set to 10 ms, using $N = 1194$. All trimmers in the circuit were adjusted to obtain a dynamic range between 0 and 10 V, and a transfer equation, with unity gain and no offset, as

$$v_{\text{out}}(t) = v_{\text{in}} \left(T_s \left\lfloor \frac{t}{T_s} - N + 1 \right\rfloor \right). \quad (7)$$

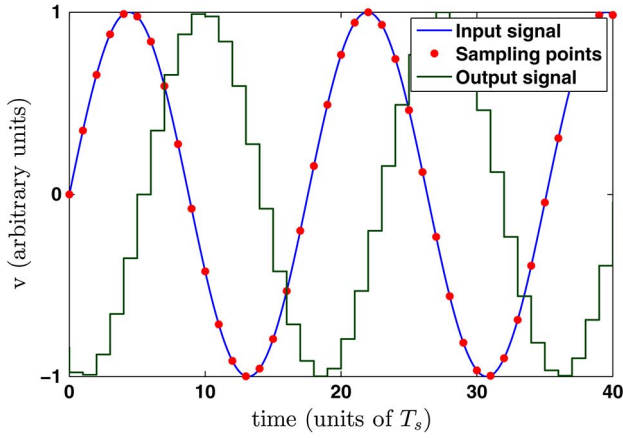


Fig. 2. Simulated examples of input and output signals and the sampling points of the BBD. The offset and gain are set null, and $N = 5$.

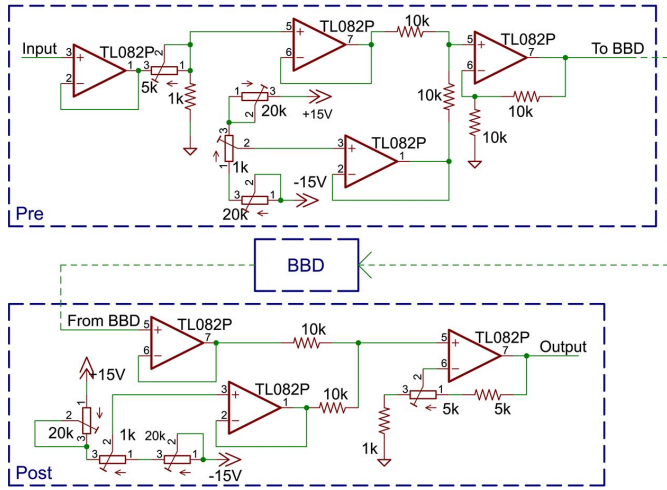


Fig. 3. Circuit schematic of the pre- and postamplification circuits of the delay block.

It is worth noting that, due to its internal clock, a certain amount of high-frequency noise is introduced by the delay block. This is the reason that explains the ordering of the blocks, in which the delay block is after the function block and immediately before the RC circuit. With this configuration, most of this noise is suppressed by the RC filter.

The function block was implemented for $n = 4$, as shown in the circuit schematics in Fig. 4. Other values of the exponent n could be similarly implemented. Assuming that all the operational amplifiers are working in the linear region, the transfer function results as in (3), by defining $\theta = k_1 a d^{1/4}$ and $\beta = k_2 b^{1/4}$, where k_1 and k_2 are constants that depend on the circuit, and a , b , and d depend on the positions of the trimmers indicated in Fig. 4. The parameter a does not depend on the dimensionless parameters that determine the evolution of the system, i.e., α and Γ , but only depends on θ that sets the amplitude of the oscillations. Therefore, a can be set to avoid all kind of saturation in the circuit, without changing the dynamical properties of the oscillations.

Integrated circuits AD633JN and AD712JN were used to implement sums, multiplications, and divisions because of their simplicity, accuracy, low noise, and low offset voltage. In Fig. 5, an input–output graph of this block is depicted and compared

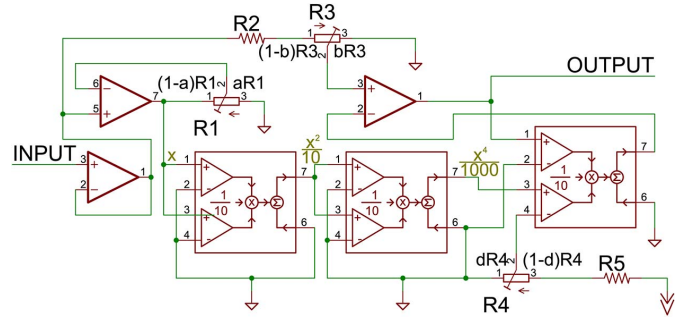


Fig. 4. Circuit schematics of the nonlinear function. Values of the resistors: $R_1 = 20 \text{ k}\Omega$, $R_2 = 56 \text{ k}\Omega$, $R_3 = 20 \text{ k}\Omega$, $R_4 = 2 \text{ k}\Omega$, $R_5 = 56 \text{ k}\Omega$.

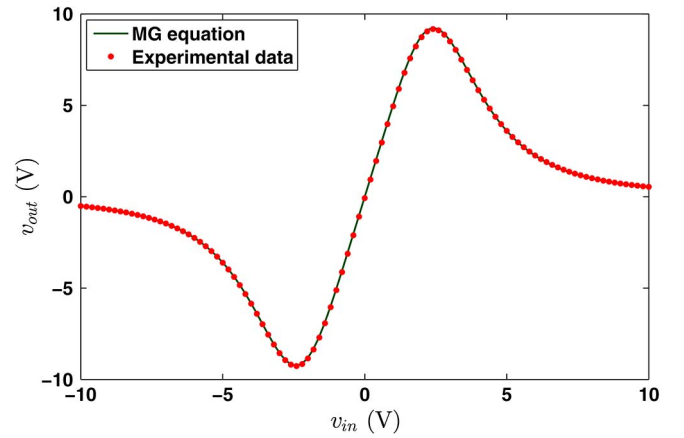


Fig. 5. Examples of the input and output of the function block (model and experiments). Parameter values: $\beta = 525 \text{ V}^4$ and $\theta = 3.19 \text{ V}$.

with (3). Although tested from -10 V to 10 V , it is used only with positive voltages, i.e., the only relevant in the MG model.

III. EFFECTIVE EQUATION

Since the delay block that we used approximates an ideal delay, the effective equation of the implemented circuit will also approximate the original MG equation. By means of the Kirchhoff's law applied to the entire circuit, we obtain

$$\frac{dv_c(t)}{dt} = \frac{1}{RC} \left[f \left(v_c \left(T_s \left[\frac{t}{T_s} - N + 1 \right] \right) \right) - v_c \right]. \quad (8)$$

The output of the delay block remains constant in each clock period; hence, it seems natural to solve (8) in steps. Let us solve it, then, for $jT_s \leq t < (j+1)T_s$ and let $v_i = v_c(iT_s)$, then

$$\frac{dv_c(t)}{dt} = \frac{1}{RC} [f(v_{j-N+1}) - v_c]. \quad (9)$$

Since $f(v_{j-N+1})$ is constant, this equation can be readily solved; the solution knowing the value of v_c in $t = jT_s$ is

$$v_c(t) = (v_j - f(v_{j-N+1})) e^{-\frac{t-jT_s}{RC}} + f(v_{j-N+1}). \quad (10)$$

Setting $t = (j+1)T_s$ and substituting the expression for $f(v)$ given in (3) results in

$$v_{j+1} = v_j e^{-\frac{T_s}{RC}} + \left(1 - e^{-\frac{T_s}{RC}}\right) \beta \frac{v_{j-N+1}}{\theta^n + v_{j-N+1}^n}. \quad (11)$$

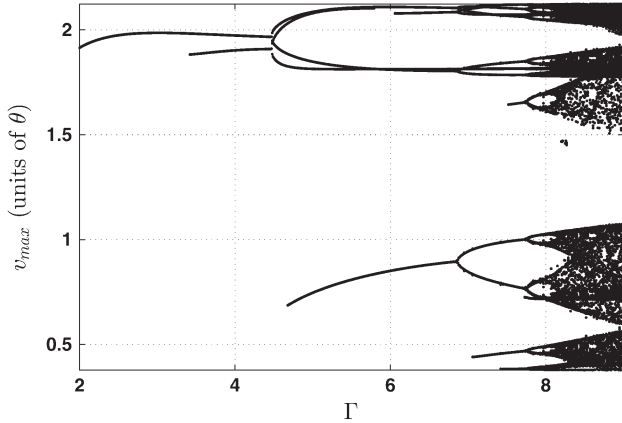


Fig. 6. Bifurcation diagram as a function of Γ in (2). Parameter values: $n = 4$ and $\alpha = 3.73$.

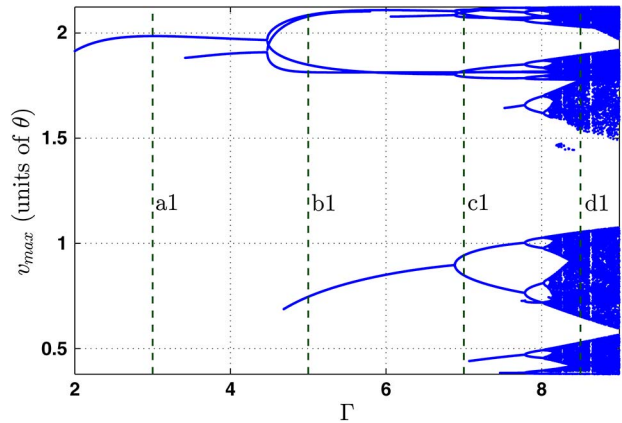


Fig. 7. Discrete-time version of the bifurcation (11) diagram shown in Fig. 6, with $N = 396$. The vertical lines labeled with a1, b1, c1, and d1 correspond to the temporal series shown in Fig. 9.

This discrete-time effective equation approaches to the original continuous-time equation (5), when N grows to infinity and the delay time $\tau = NT_s$ is kept constant.

IV. SIMULATIONS AND RESULTS

To compare the solutions of the original (continuous-time) model with the effective (discrete-time) model, we performed simulations of both, with the same parameters values. The original equation was simulated using a fifth-order Runge–Kutta scheme with variable time step.

To compare the analytical with experimental results, bifurcation diagrams were obtained by plotting the maxima of the temporal series, as a function of Γ . Such diagrams are shown in Figs. 6 and 7, for simulations of the original and the effective equation, respectively, while experimental results are shown in Fig. 8. We can observe great agreement in all cases. The familiar, i.e., already present in ODEs, period-doubling branches and chaotic behavior can be appreciated as the control parameter Γ is increased. In addition, the three bifurcation diagrams present the typical characteristics of DDEs [3], for instance, singles branches that appear (*out of the blue*) or disappear for certain control parameter values.

Some examples of time series with different Γ values are shown in Fig. 9, corresponding to the values indicated by

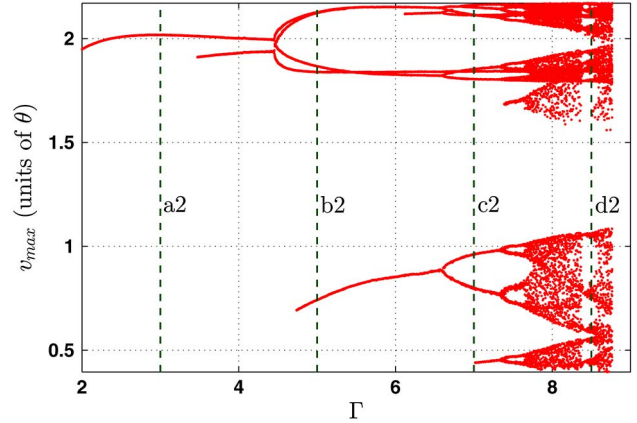


Fig. 8. Experimental bifurcation diagram using the same parameter values as in Figs. 6 and 7, for $N = 1194$.

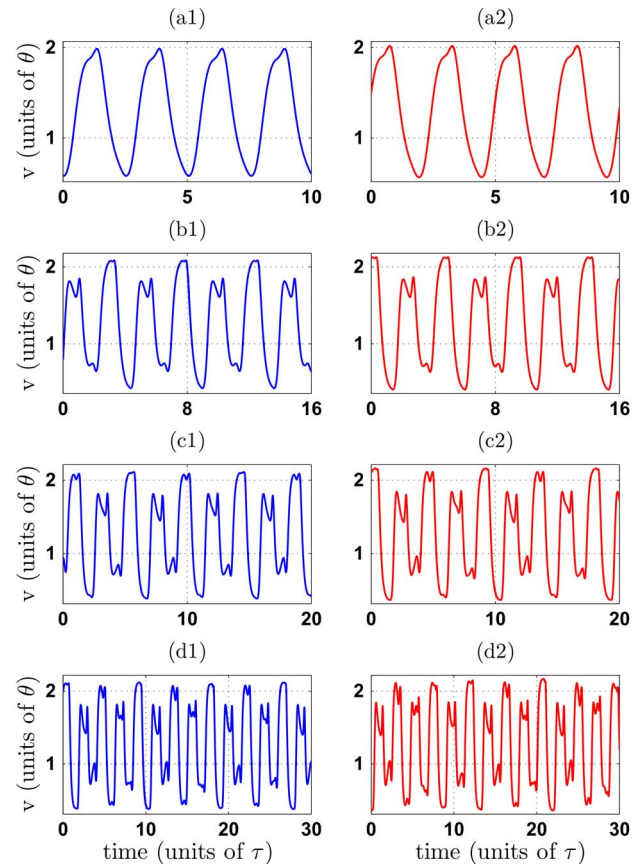


Fig. 9. Exemplary temporal evolutions of the MG model: (left) simulations using (11) and (right) experiments. Parameter values: (a) $\Gamma = 3$, (b) $\Gamma = 5$, (c) $\Gamma = 7$, and (d) $\Gamma = 8.5$. The maxima of the cross-correlation functions between numerical and experimental time series for the three periodic cases (a), (b), and (c) are 0.999, 0.966, and 0.923, respectively.

vertical dashed lines in Figs. 7 and 8. The maxima of the time series correspond to the intersections of these vertical lines and the bifurcation diagrams. These time series also show a great deal of concordance between experimental and simulated data. The first presented waveforms (a1 and a2) correspond to a simple oscillation with only one peak per period. Increasing the time delay Γ after new peak appearances and a bifurcation, a more complex waveform, with longer period and five peaks per period, is observed (b1 and b2). With additional increases in the

time delay, more peaks per period and longer periods appear, as shown in *c1* and *c2*. Finally, chaotic behavior, in agreement with the previous works [1], [3], [16], is seen in *d1* and *d2*.

To verify the accuracy of the implementation, we calculated the cross-correlation functions between numerical and experimental time series, corresponding to the periodic regimes shown in the left and right columns in Fig. 9, respectively. As the time series are not aligned, the maximum of the cross-correlation function corresponds to the time lag, in which the signals are in phase. The quantitative estimators of the similarity, given by the maximum value indicated in the caption, reveal an excellent agreement between experimental and numerical data.

V. CONCLUSION AND PERSPECTIVES

The MG model was simulated using an electrical analog. The results of simulations of the original equation were compared with the discrete equation and with the experimental data. Our novel approach to implement the nonlinear function and delay blocks exhibits several advantages compared with previous implementations.

One remarkable advantage is that a precise equation for the discrete-time evolution can be easily obtained, due to the exact transfer function of the delay block and the nonlinear function. Then, it is possible to write down and solve the discrete equations and, then, corroborate the quality of the experimental setup. This is in contrast to other approaches using piecewise linear functions. In addition, the parameter n is exactly determined by means of multipliers and divisors.

The implementation of the delay is also advantageous. The BBD device avoids digitalizing the signal from the RC circuit, applying the delay, and converting back to the analog domain. This is at odds with previous implementations using analog delay lines. Moreover, the ordering of the blocks, which is usually ignored, played an important role in getting the most out of the delay block and allowed to suppress most of the electrical noise in the experimental data.

According to the value of the time delay, the system exhibits a wide variety of behaviors, including fixed, periodic waveform with different numbers of peaks per period, and, finally, aperiodic or chaotic solutions. The great agreement between experimental and numerical results suggests that deeper understanding of the dynamics of the MG model can be obtained using our implementation. In addition, due to the simplicity and versatility, this approach could be extended to other time-delayed systems.

REFERENCES

- [1] M. C. Mackey and L. Glass, "Oscillation and chaos in physiological control systems," *Science*, vol. 197, no. 4300, pp. 287–289, Jul. 1977.
- [2] M. A. De Menezes and R. Z. Dos Santos, "The onset of Mackey–Glass leukemia at the edge of chaos," *Int. J. Modern Phys. C*, vol. 11, no. 8, pp. 1545–1553, 2000.
- [3] L. Junges and J. A. Gallas, "Intricate routes to chaos in the Mackey–Glass delayed feedback system," *Phys. Lett. A*, vol. 376, no. 30, pp. 2109–2116, Jun. 2012.
- [4] S. Sano, A. Uchida, S. Yoshimori, and R. Roy, "Dual synchronization of chaos in Mackey–Glass electronic circuits with time-delayed feedback," *Phys. Rev. E*, vol. 75, no. 1, Jan. 2007, Art. ID. 016207.
- [5] A. Wan and J. Wei, "Bifurcation analysis of Mackey–Glass electronic circuits model with delayed feedback," *Nonlinear Dyn.*, vol. 57, no. 1/2, pp. 85–96, Jul. 2009.
- [6] P. Grassberger and I. Procaccia, "Measuring the strangeness of strange attractors," *Phys. D: Nonlinear Phenom.*, vol. 9, no. 1, pp. 189–208, Oct. 1983.
- [7] A. Namajūnas, K. Pyragas, and A. Tamaševičius, "Stabilization of an unstable steady state in a Mackey–Glass system," *Phys. Lett. A*, vol. 204, no. 3, pp. 255–262, Aug. 1995.
- [8] J. D. Farmer and J. J. Sidorowich, "Predicting chaotic time series," *Phys. Rev. Lett.*, vol. 59, no. 8, pp. 845–848, Aug. 1987.
- [9] E. A. Wan and R. Van Der Merwe, "The unscented Kalman filter for nonlinear estimation," in *Proc. IEEE AS-SPCC*, 2000, pp. 153–158.
- [10] M. Tateno and A. Uchida, "Nonlinear dynamics and chaos synchronization in Mackey–Glass electronic circuits with multiple time-delayed feedback," *Nonlinear Theory Appl., IEICE*, vol. 3, no. 2, pp. 155–164, 2012.
- [11] A. Fowler, "Respiratory control and the onset of periodic breathing," *Math. Modelling Nat. Phenom.*, vol. 9, no. 1, pp. 39–57, Jan. 2014.
- [12] T. Zhang, "Almost periodic oscillations in a generalized Mackey–Glass model of respiratory dynamics with several delays," *Int. J. Biomath.*, vol. 7, no. 3, 2014, Art. ID. 1450029.
- [13] C.-H. Yang, Y.-T. Wong, S.-Y. Li, and C.-M. Chang, "Robust chaos lag synchronization and chaos control of double Mackey–Glass system by noise excitation of parameters," *J. Comput. Theoretical Nanosci.*, vol. 10, no. 1, pp. 218–226, Jan. 2013.
- [14] J. Soto, P. Melin, and O. Castillo, "Optimization of interval type-2 fuzzy integrators in ensembles of ANFIS models for prediction of the Mackey–Glass time series," in *Proc. IEEE Conf. Norbert Wiener 21CW*, 2014, pp. 1–8.
- [15] Y. L. Ning, X. Y. Wang, and X. P. He, "Study on prediction of Mackey–Glass chaotic time series using support vector machines," in *Proc. Adv. Mater. Res.*, 2014, vol. 1051, pp. 1009–1015.
- [16] A. Namajūnas, K. Pyragas, and A. Tamaševičius, "An electronic analog of the Mackey–Glass system," *Phys. Lett. A*, vol. 201, no. 1, pp. 42–46, May 1995.
- [17] A. Kittel, J. Parisi, and K. Pyragas, "Generalized synchronization of chaos in electronic circuit experiments," *Phys. D, Nonlinear Phenom.*, vol. 112, no. 3, pp. 459–471, Feb. 1998.
- [18] M.-Y. Kim, C. Sramek, A. Uchida, and R. Roy, "Synchronization of unidirectionally coupled Mackey–Glass analog circuits with frequency bandwidth limitations," *Phys. Rev. E*, vol. 74, no. 1, 2006, Art. ID. 016211.
- [19] T. M. Hoang, T. D. Nguyen, N. V. Duc, J. C. Chedjou, and K. Kyamakyia, "Design and simulation of circuit for synchronization of multidelay feedback systems," in *Proc. 15th ISTET*, 2009, pp. 1–4.
- [20] V.-T. Pham, L. Fortuna, and M. Frasca, "Implementation of chaotic circuits with a digital time-delay block," *Nonlinear Dyn.*, vol. 67, no. 1, pp. 345–355, Jan. 2012.